DETAILED AND GLOBAL CHEMICAL KINETICS MODEL FOR HYDROGEN

N.M. Marinov, C.K. Westbrook and W.J. Pitz
Lawrence Livermore National Laboratory
P.O. Box 808, L -298 , Livermore, CA. 94551, USA

ABSTRACT

Detailed and global chemical kinetic computations for hydrogen-air mixtures have been performed to describe flame propagation, flame structure and ignition phenomena. Simulations of laminar flame speeds, flame compositions and shock tube ignition delay times have been successfully performed. Sensitivity analysis was applied to determine the governing rate-controlling reactions for the experimental data sets examined. In the flame propagation and structure studies, the $OH + H_2 = H_2O + H$, $O + H_2 = OH + H$ and $O + OH = O_2 + H$ reactions were the most important in flames. The shock tube ignition delay time study indicated the $H + O_2 + M = HO_2 + M$ ($M = N_2$, H_2) and $O + OH = O_2 + H$ reactions controlled ignition. Also, a global rate expression for a one step overall reaction was developed and validated against experimental hydrogen-air laminar flame speed data. The global reaction expression for the single step reaction $H_2 + 1/2O_2 = H_2O$ at one atmosphere was determined to be

$$k_{global} = 1.8 \times 10^{13} \exp(-17614K / T) [H_2]^{1.0} [O_2]^{0.5}$$

INTRODUCTION

The public concern for improved urban air quality, finite fossil fuel resources, and global warming trends support the need for a clean burning alternative fuel. Hydrogen is an attractive alternative fuel, because it does not produce CO_2 greenhouse gas, offers the potential of reduced NO_x pollutant emissions, can enhance fuel economy when used in hydrocarbon mixtures and is virtually limitless in supply.

Hydrogen as a fuel is unique because of its simple oxidation kinetics, very fast mass diffusivity and low molecular weight. Interestingly, all chemical reactions that consume molecular hydrogen in the H_2 - O_2 system produce atomic hydrogen which is an extremely reactive and diffusive species. The hydrogen atom is the most important radical needed for flame propagation and ignition in virtually all combustion systems.

The purpose of this paper is to describe the reaction kinetics for hydrogen combustion which is suitable for describing flame propagation, flame composition measurements and ignition delay times. A detailed reaction mechanism was developed and validated against laminar flame speeds for a wide range of hydrogen - air stoichiometries, flame structure measurements of a low pressure rich H_2 /O_2 /Ar laminar flame and shock tube ignition delay times near the second explosion limit. In addition, a one-step global rate expression for the single step reaction

$H_2 + 1/2O_2 = H_2O$ was developed and validated against laminar flame speed data.

REACTION MECHANISM

The detailed reaction mechanism used in this study is given in Table 1. The reverse rate constants are calculated from the forward rate constants through the equilibrium rate constants derived from the CHEMKIN thermochemical database [11]. The chemical kinetic reaction rates used for the H_2 - O_2 chain branching / propagating submechanism (reactions 1- 4) are well known and are considered to be accurate to within a factor of 1.5 for the 300 K - 2500 K temperature range. The H_2 - O_2

Table 1. H_2 / O_2 / N_2 / Ar reaction mechanism

Units are cm^3 - mole - sec - kcal - K ; $k = A\ T^n \exp(-E_a/RT)$

No.	Reaction	ΔH^o_{298K}	A_{fwd}	n_{fwd}	$E_{a,fwd}$	Reference
1.	$O + OH = O_2 + H$	-16.77	2.02E+14	-0.40	0.0	Masten et al. [1]
2.	$OH + H_2 = H + H_2O$	-15.01	2.14E+08	1.52	3.449	Michael et al. [2]
3.	$OH + OH = O + H_2O$	-16.88	3.57E+04	2.40	-2.112	Wooldridge [3]
4.	$O + H_2 = OH + H$	1.85	5.06E+04	2.67	6.290	Sutherland [4]
5a.	$H + H + M = H_2 + M^{(a,b)}$	-104.2	1.00E+18	-1.00	0.0	Dixon-Lewis [5]
5b.	$H + H + H_2 = H_2 + H_2$	-104.2	9.27E+16	-0.60	0.0	Dixon-Lewis [5]
5c.	$H + H + H_2O = H_2 + H_2O$	-104.2	6.00E+19	-1.25	0.0	Dixon-Lewis [5]
6.	$O + O + M = O_2 + M$	-119.1	1.89E+13	0.00	-1.788	Tsang et al. [6]
7.	$O + H + M = OH + M$	-102.3	4.71E+18	-1.00	0.0	Tsang et al. [6]
8.	$H + OH + M = H_2O + M$	-119.2	2.21E+22	-2.00	0.0	Tsang et al. [6]
9a.	$H + O_2 + M = HO_2 + M^{(c)}$	-49.6	k_o = 1.05E+19 $T^{-1.257}$			Compiled Fit [d, e]
			k_∞ = 4.517E+13			Cobos et al. [7]
9b.	$H + O_2 + H_2 = HO_2 + H_2$	-49.6	k_o = 1.52E+19 $T^{-1.133}$			Compiled Fit [d, f]
			k_∞ = 4.517E+13			Cobos et al. [7]
9c.	$H + O_2 + N_2 = HO_2 + N_2$	-49.6	k_o = 2.031E+20 $T^{-1.590}$			Compiled Fit [d, f]
			k_∞ = 4.517E+13			Cobos et al. [7]
9d.	$H + O_2 + H_2O = HO_2 + H_2O$	-49.6	k_o = 2.10E+23 $T^{-2.437}$			Compiled Fit [d]
			k_∞ = 4.517E+13			Cobos et al. [7]
10.	$HO_2 + H = H_2 + O_2$	-54.6	8.45E+11	0.65	1.241	Compiled Fit [d]
11.	$HO_2 + H = OH + OH$	-35.97	1.50E+14	0.00	1.000	Warnatz [8]
12.	$HO_2 + H = O + H_2O$	-52.85	3.01E+13	0.00	1.721	Baulch et al. [9]
13.	$HO_2 + O = OH + O_2$	-51.73	3.25E+13	0.00	0.000	Baulch et al. [9]
14.	$HO_2 + OH = H_2O + O_2$	-69.61	2.89E+13	0.00	-0.497	Baulch et al. [9]
15.	$HO_2 + HO_2 = H_2O_2 + O_2$	-37.53	k = 4.20E+14exp(-11.98/RT) + 1.30E+11exp(+1.629/RT)			Hippler et al. [10]
16.	$OH + OH + M = H_2O_2 + M^{(g)}$	-51.14	k_∞ = 1.24E+14 $T^{-0.37}$			Compiled Fit [d]
			k_o = 3.041E+30 $T^{-4.63}$ exp(-2.049/RT)			
	$<\Delta E_{down}>$=850cm^{-1},M = Ar, Troe Parameters /a=0.47 T***=100. T*=2000. T**=1.E+15/					
17.	$H_2O_2 + H = H_2O + OH$	-68.05	3.07E+13	0.00	4.217	Baulch et al. [9]
18.	$H_2O_2 + H = HO_2 + H_2$	-17.07	1.98E+06	2.00	2.435	Compiled Fit [d]
19.	$H_2O_2 + O = OH + HO_2$	-15.20	9.55E+06	2.00	3.970	Tsang et al. [6]
20.	$H_2O_2 + OH = H_2O + HO_2$	-32.08	2.40E+00	4.042	-2.162	Compiled Fit [d]

a) $[M] = \sum \varepsilon_i [c_i]$ where ε_i represents the chaperon efficiency and $[c_i]$ represents the concentration of the i^{th} species. b) $\varepsilon_{H2} = 0.0$; $\varepsilon_{H2O} = 0.0$ and all other species have efficiencies equal to unity. c) $\varepsilon_{H2} = 0.0$; $\varepsilon_{H2O} = 0.0$; $\varepsilon_{N2} = 0.0$ and all other species have efficiencies equal to unity. d) See text for description of the reaction rate expression fit. e) See Figure 1 f) See Figure 2 g) Troe fall - off reaction form: $F_{cent} = (1 - a) \exp(-T/T^{***}) + a \exp(-T/T^{*}) + \exp(-T^{**}/T)$

dissociation / recombination reactions have been critically reviewed by Dixon - Lewis [5], Tsang and Hampson [6], and Yetter et al. [12]. Reactions 5, 6, and 8 are accurate to within a factor of 2, and reaction 7 is accurate to a factor of 10. Greater uncertainty in the kinetics exists for those reactions which form or consume HO_2 radicals and H_2O_2. A detailed review of the chemical kinetics literature was performed to critically evaluate these reactions.

In Figs. 1 and 2, the $H + O_2 + M = HO_2 + M$ (M = any third body) reaction was evaluated over the 300 K - 2500 K temperature range. The $H + O_2 + M = HO_2 + M$ (M = Ar) reaction was primarily fit to the measurements of Wong and Davis [13], Carleton et al. [14], Hsu et al. [15], Pirraglia et al. [16], Gay and Pratt [17], and Pamidimukkala and Skinner [18]. The $H + O_2 + H_2 = HO_2 + H_2$ reaction was fitted to the data of Nielsen et al. [20] and Kochubei and Moin [21]. The $H + O_2 + N_2 = HO_2 + N_2$ reaction was fitted primarily to the studies of Hsu et al. [15], Slack [22] and Peeters et al. [23]. These resulting fits are within the uncertainty factor of three prescribed to the Baulch recommended rates involving these reactions for the 300 K - 2000 K temperature range [9]. The kinetic rate applied to the $H + O_2 + H_2O = HO_2 + H_2O$ reaction was derived from using the fitted rate of reaction 9a and then using the Hsu et al. [14] relation of $k_{H2O} / k_{He} = 23.9 (T / 300)^{-1.18}$ (assuming M = He = Ar) for the 298K - 635K temperature range. Discrepancies in the literature values for third body efficiencies of H_2O at temperatures greater than 1000K makes the kinetic rate for reaction 9d suspect to error. However, the fitted kinetic rate for this reaction agrees, to within a factor of two, with the Baulch recommendation in the 1000 K - 2000 K temperature range.

The kinetic rate for $H + HO_2 = H_2 + O_2$ was fitted to the low temperature measurements of Keyser [24], intermediate temperature measurements of Baldwin and Walker [25], and to the reverse rate of this reaction at high temperatures as determined by Koike [26]. The $OH + OH (+M) = H_2O_2 (+M)$ reaction was fitted by using a complex set of rate parameters in the Troe fall-off formulation [27]. This complex fit was validated against the experimental measurements of Zellner et al. [28], Troe [29, 30], Brouwer et al. [31] and Basevich et al. [32]. The $H_2O_2 + H = HO_2 + H_2$ reaction was fitted to a T^2 expression (analogous to the H-atom

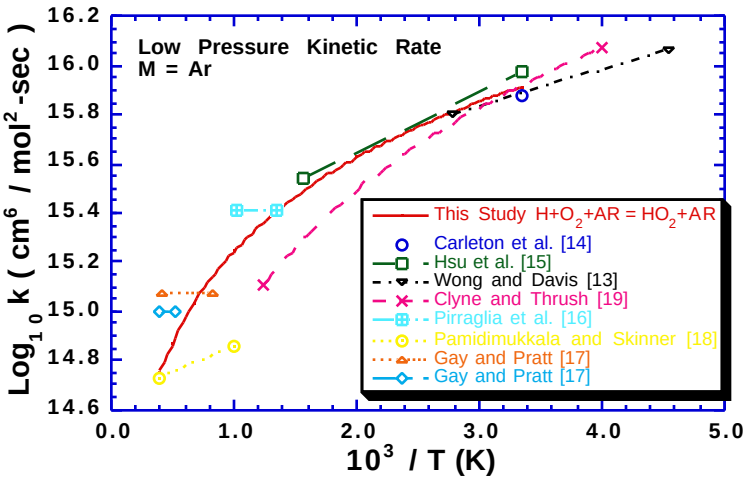

Figure 1. An Arrhenius plot for H + O_2 + M = HO_2 + M reaction, M = Ar. Data from references [13 - 19] were used to generate the curve fit.

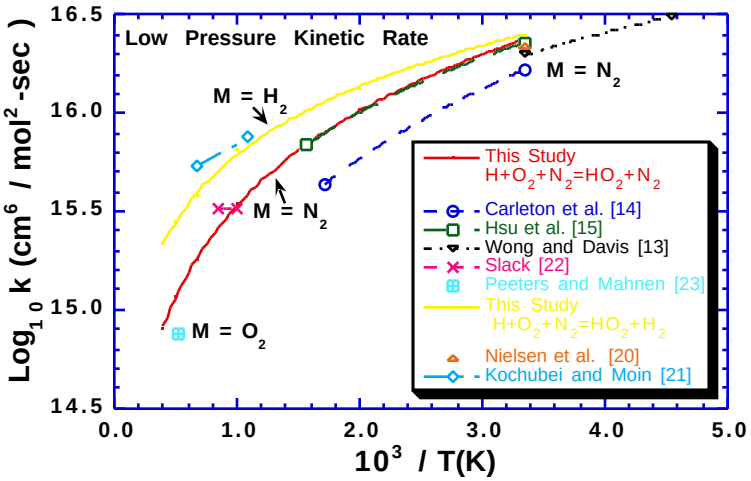

Figure 2. Arrhenius plots for H + O_2 + H_2 = HO_2 + H_2 and H + O_2 + N_2 = HO_2 + N_2. Data from references [20, 21] were used to generate the curve fit to H + O_2 + H_2 = HO_2 + H_2. Data from references [15, 22, 23] were used to generate the curve fit to H + O_2 + N_2 = HO_2 + N_2.

abstraction reaction H_2O_2 + O = OH + HO_2) by using the data of Albers et al. [33], and Baldwin and Walker [25]. The H_2O_2 + OH = H_2O + HO_2 reaction was primarily fitted to the measurements of Hippler and Troe [34], Baldwin et al. [35, 36], Kurylo et al. [37], and Keyser [38].

REACTION KINETICS OF H_2 - AIR LAMINAR FLAME SPEEDS

Recent experimental data [39 - 46] for the laminar flame speed (S_L) of atmospheric H_2 - Air mixtures have been compiled and are shown in figures 3 and 4. In figure 3, a ~70 cm/sec variation in S_L around Φ (H_2 fuel to air equivalence ratio) of 1.4 is exhibited, while in figure 4, considerable scatter by as much as ~60 cm/sec in S_L is found for lean hydrogen mixtures. The observed discrepancies in the H_2 - Air laminar flame speeds is due to aerodynamic flame strain (or stretch). Aerodynamic flame strain is caused by preferential mass and thermal diffusion, and flow divergence [47, 48]. Experimental data uncorrected for these effects represent a strain dependent flame speed and *not* the true (strain-free) laminar flame speed (S_L). This study has modeled the flame strain corrected experimental data for H_2 - Air laminar flame speeds at one atmosphere. A one-dimensional, premixed, laminar flame code (PREMIX) [47] was used to perform the computations with the detailed H_2 /O_2 /N_2 /Ar mechanism and transport [50]. Numerical computations were performed using multi-component mass transport and thermal diffusion for equivalence ratios greater than 0.6. Mixture averaged transport properties were used at equivalence ratios less than or equal to 0.6 so that a numerically converged solution could be obtained.

Numerical calculations show good agreement with the experimental laminar flame speed data for the full range of hydrogen-air stoichiometries (figure 3). A laminar flame speed maximum of 300cm/sec at an equivalence ratio of 1.6 and atmospheric pressure was calculated, also in agreement with the measured data.

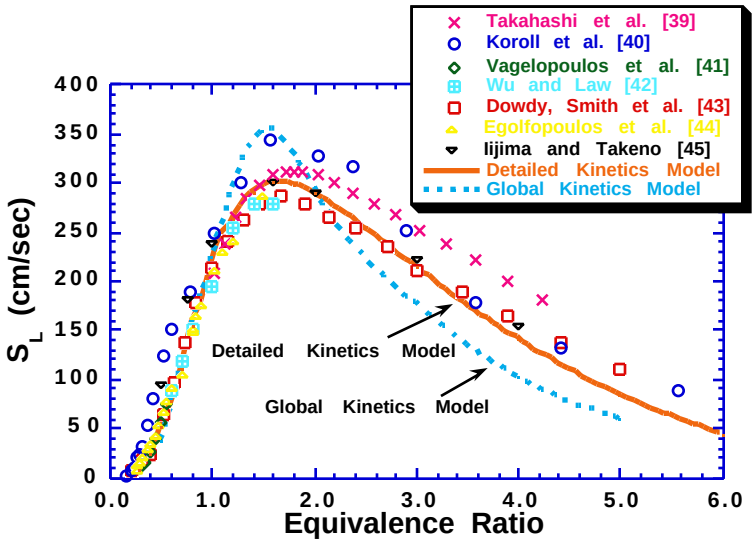

Figure 3. Hydrogen -air laminar flame speeds at 1 atmosphere and T_u = 298K as a function of equivalence ratio. Equivalence ratio range is 0.15 to 6.0. Comparison between experimental data [39 - 45] (symbols) and computations (detailed model - solid line, global model - dashed line).

In addition, computations performed at equivalence ratios of 0.4, 1.0 and 4.0 predict flame speed values of 24.3 cm/sec, 210 cm/sec, and 144 cm/sec, all of which are good.

A sensitivity analysis of the important chemical reactions which influence the mass burning rate (or the laminar flame speed) was performed at equivalence ratios of 0.6, 1.0 and 1.4. The results are shown in figure 5. The normalized sensitivity coefficient was calculated through the expression,

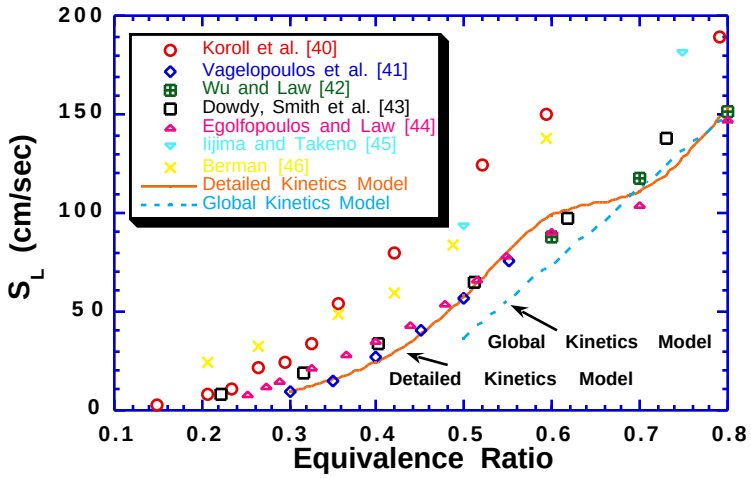

Figure 4. Hydrogen -air laminar flame speeds at 1 atmosphere and T_u = 298K as a function of equivalence ratio. Equivalence ratio range is 0.15 to 0.80. Comparison between experimental data [40 - 46] (symbols) and computations (detailed model - solid line, global model - dashed line).

$$(A_i / m_L) (\Delta m_L / \Delta A_i) \qquad (1)$$

where A_i is the pre-exponential factor of the i^{th} reaction rate expression and m_L is mass burning rate (where $m_L = \rho_u S_L$, ρ_u is the unburned gas density). The results show that the dominant reactions promoting flame propagation are $OH + H_2 = H_2O + H$, $O + OH = O_2 + H$, $H + HO_2 + OH + OH$ and $O + H_2 = OH + H$. The dominant reaction retarding flame propagation is $HO_2 + H = H_2 + O_2$.

As the H_2-Air stoichiometry goes from rich to lean, the laminar flame speed becomes less sensitive to $H + O_2 = OH + O$ and more sensitive to reactions involving the HO_2 radical and O-atom. The forward reaction in $H + O_2 = OH + O$ is endothermic and therefore its chemical kinetic rate is especially sensitive to temperature changes as hydrogen mixtures become leaner. The HO_2 radical, primarily formed by $H + O_2 + M = HO_2 + M$ (M = any third body), is readily produced in the preheat zone and is principally consumed by H-atoms to produce OH radicals. The O-atom, primarily formed by $H + O_2 = OH + O$, reacts with H_2 in the flame zone to produce OH and H-atom. These reactions control the OH radical production needed for the important flame propagation step, $OH + H_2 = H_2O + H$.

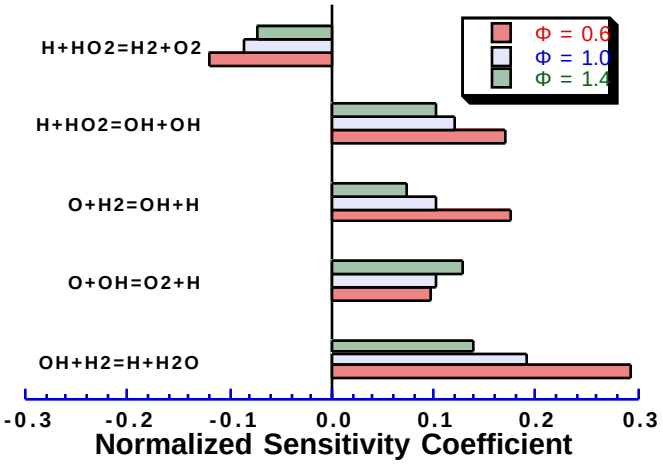

Figure 5. Sensitivity analysis of hydrogen - air laminar flame speeds at 1 atmosphere and T_u = 298K. Normalized first order sensitivity coefficients given by $(A_i / m_L) (\Delta m_L / \Delta A_i)$.

While detailed reaction mechanisms provide insight into flame structure and reactivity of gas mixtures, there is a great need for one-step global kinetics for use in complex fluid mechanics codes that utilize two- to three-dimensional geometry. The computational effort of using detailed kinetics in such models is not practical. Therefore, a one-step overall reaction was developed and validated against laminar flame speed data. The global reaction study made use of the HCT code [51] for the laminar flame speed computations. The global reaction rate parameters were varied in order to obtain good agreement between computed and experimentally observed flame speeds. The global rate expression at one atmosphere for the single step reaction $H_2 + 1/2\ O_2 = H_2O$ was determined to be

$$k_{global} = 1.8 \times 10^{13} \exp(-17614K / T) [H_2]^{1.0} [O_2]^{0.5} \qquad (2)$$

Figures 3 and 4 shows the comparison of the experimentally measured laminar flame speeds with the computed ones using the global reaction model. The predicted flame speed well represented the experimental data for only the 0.60 - 1.1 equivalence ratio range. Predictions by the global reaction model were considered poor outside this equivalence ratio range. The poor prediction is attributed to chemical and thermal structure changes in the flame as the stoichiometry varies which could not be properly accounted for in the global reaction model.

REACTION KINETICS OF A LOW PRESSURE RICH H_2 - O_2 - AR FLAME

While comparison with laminar flame speed data is a valuable test of a detailed reaction mechanism, a more demanding validation method is to compare experimental flame structure data with numerical computations. The structure of a low pressure rich H_2 /O_2 /Ar laminar flame investigated by Vandooren and Bian

[52] was used to validate the chemical kinetic model. These experimental measurements were performed at a pressure of 35.5 torr (0.047 atm) which differed from the laminar flame speed measurements performed at 1 atmosphere. This large difference in pressure allowed the two body reactions in the detailed mechanism to be tested at these conditions.

The experimental data were obtained using a premixed, flat flame burner. The composition of the incoming reactants was 39.7% H_2, 10.3% O_2 and 50% Ar (equivalence ratio of 1.91) and had an in flow velocity of 131 cm/sec. Flame structure measurements were performed by molecular beam sampling with a mass spectrometer. Measurement errors of the stable compounds (H_2, O_2, H_2O) were estimated to be ca. 2% and for radicals (OH, O-atom, H-atom) ca. 10%. Computations were performed using the PREMIX code with the measured temperature profile as given in the reference [52].

Figure 6 shows the comparison of the experimental mole fraction profiles of the stable species with the computed ones. The predicted molecular hydrogen profile agreed very well with the measured profile. About 40% of the initial hydrogen was predicted to remain in the burnt gases, in good agreement with the experimental results. The predicted profile for the molecular oxygen mole fraction agreed well with the data. However, there exists some discrepancy between the model and the experimental data for O_2 in the preheating zone of the flame close to the burner. The experimental and computed maximum concentrations of water were identical and both profiles exhibited the same gradient of H_2O formation. If the experimental profile for water was shifted by approximately 0.5 mm towards the burner surface, better agreement would result. Reaction flux analysis was applied to this flame and determined that H_2 was destroyed a factor of two faster by reaction 2 than reaction 4. The O_2 was primarily removed by reaction 1 with secondary reactions 9a and 9b playing a minor role. Water was formed exclusively from reaction 2.

Figure 7 shows the comparison of the experimental mole fraction profiles of the radical species with the computed ones. For all three radical species, the model predictions are somewhat higher than the measured values. The computed profile for the hydroxyl radicals exhibited the same profile behavior as the experimental measurements, however the detailed kinetic model overestimated the hydroxyl concentration by a factor of 1.75 - 2.0 at the peak OH level and in the post-flame

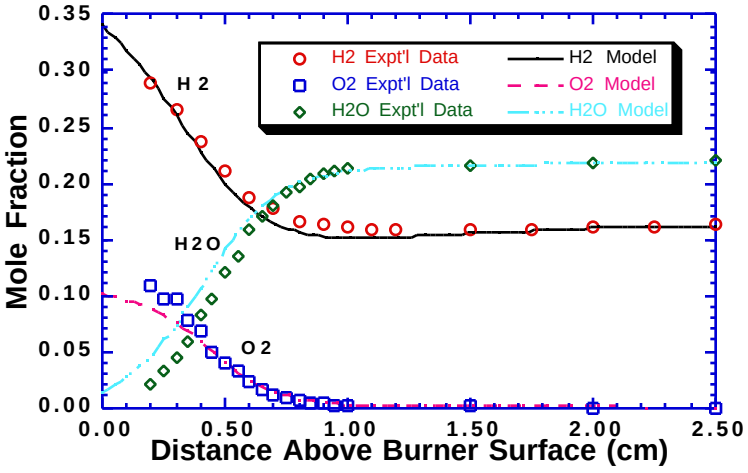

Figure 6. Rich Hydrogen-Oxygen-Argon Flame [52] of the inlet composition 39.7% H_2 , 10.3% O_2, and 50.0% Ar (Φ = 1.91 equivalence ratio). Comparison between computations (lines) and experimental data for H_2 , O_2 and H_2O (symbols).

zone. The location of the predicted maximum for the O-atom corresponds well with experimental data. The model overpredicted the O-atom concentration by a factor of 1.7 - 2.0 in the flame and post-flame zones. The model overpredicted the H-atom concentration by ~60% at the peak H-atom level and predicted to within a factor of two the H-atom concentration in the post-flame zone. Model predictions for the radical species were worse in the preheat zone of the flame with the H-atom over-

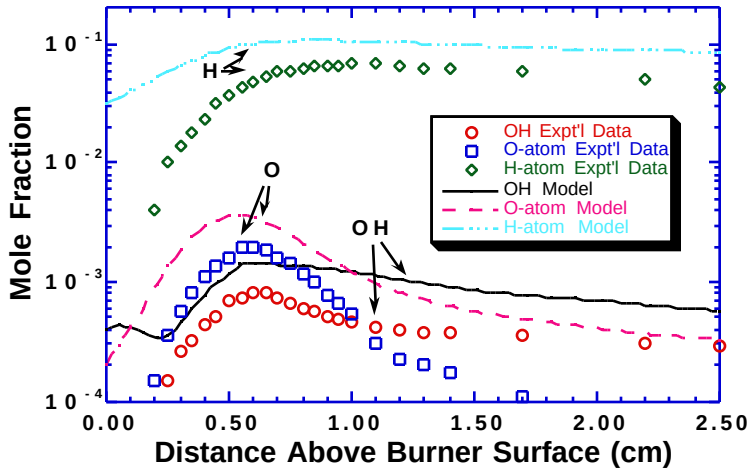

Figure 7. Rich Hydrogen-Oxygen-Argon Flame [52] of the inlet composition 39.7% H_2 , 10.3% O_2, and 50.0% Ar (Φ = 1.91 equivalence ratio). Comparison between computations (lines) and experimental data for OH , O-atom and H-atom (symbols).

predicted by a factor of five. The HO_2 concentration was not measured in this flame but the model predicted a peak HO_2 mole fraction of 7.5×10^{-6} at ca. 0.05mm downstream from the burner surface. Reaction flux analysis was applied to this flame and determined that the OH radical was primarily produced by reactions 1 and 4 and destroyed by reaction 2, while in the preheat zone OH was also formed by reaction 11. The O-atom was produced by reaction 1 and destroyed by reaction 4. The H-atom was produced a factor of two faster by reaction 2 than reaction 4, while H-atom was removed by reaction 1. The HO_2 radical was formed a factor of two faster by reaction 9b than reaction 9a, while reaction 11 consumed HO_2 a factor of three faster than reaction 10.

The predicted stable species profiles agreed very well with the measured profiles. However, the H, O and OH radical concentration was overpredicted by approximately a factor of two. This study did not consider wall destruction of the free radicals within the sample probe which could explain the discrepancy between the numerically predicted and experimentally measured free radical concentrations.

REACTION KINETICS OF SHOCK TUBE IGNITION DELAY TIMES

The shock tube experimental data of Slack [22] was used to test the present H_2 /O_2 /N_2 /Ar mechanism for ignition delay near the second explosion limit. Stoichiometric hydrogen-air mixtures were heated by reflected shock waves at 2 atmospheres and for the 980K - 1176K reflected shock temperature range. Numerical simulations were performed with the SENKIN code [53] assuming that the gas dynamics behaves in an adiabatic constant volume process.

In figure 8, the ignition delay data of Slack are compared to the numerical computations. For temperatures below ca. 1025K, the experimental ignition delay times become significantly longer as the experimental conditions approach the second explosion limit (classically defined as $2\ k_{rev,1} / k_{9a,b,c,d} = [M]$). The

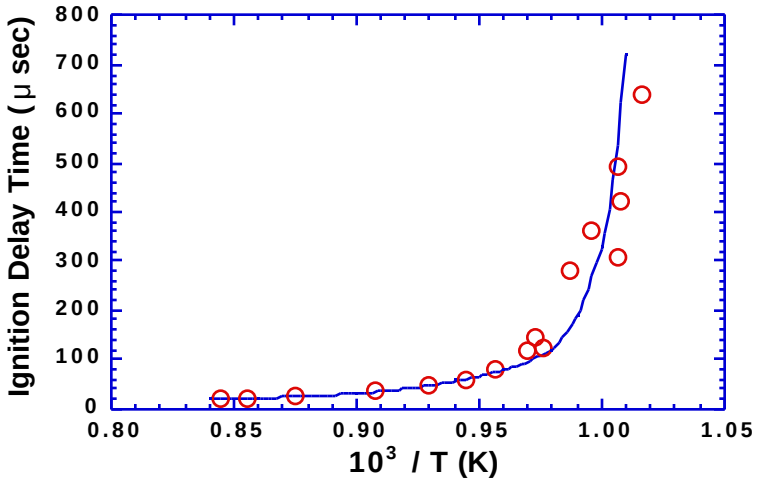

Figure 8. Ignition delay times of stoichiometric hydrogen - air at 2 atmospheres. Comparison between experimental data [22] (circles) and computations (lines).

Table 2. Sensitivity analysis of computed ignition delay times

No.	Reaction	ln (t_{ign}(perturbed) / t_{ign}(baseline)) 1000K	1111K
9b.	$H + O_2 + H_2 = HO_2 + H_2$	3.03	0.18
9c.	$H + O_2 + N_2 = HO_2 + N_2$	3.03	0.18
1.	$O + OH = O2 + H$	-1.67	-0.61
9a.	$H + O_2 + M = HO_2 + M^a$	0.48	0.04
11.	$HO_2 + H = OH + OH$	-0.13	-0.02
4.	$O + H_2 = OH + H$	-0.09	-0.08
10.	$HO_2 + H = H_2 + O_2$	0.08	-0.02
8.	$H_2O_2 + H = HO_2 + H_2$	-0.03	0.00
2.	$OH + H_2 = H + H_2O$	-0.02	-0.02
12.	$HO_2 + H = O + H2O$	-0.02	-0.01
13.	$HO_2 + O = O_2 + OH$	0.01	0.00

[a]M = any third body except N_2, H_2 and H_2O.

detailed chemical model predicted the same behavior. For temperatures above ca. 1100K, the ignition delay time is shorter and is predicted correctly by the model.

A sensitivity analysis of the important chemical reactions which influence the ignition delay time was conducted at temperatures of 1000K and 1111K. The results are shown in Table 2. In the sensitivity analysis, the pre-exponential factor, A, for each reaction was perturbed upward by a factor of 2 while maintaining the same equilibrium rate constant. The ignition delay was then computed at the same experimental conditions as the baseline case. The sensitivity coefficient values shown in Table 2 are represented by the expression:

$$\ln (t_{ign}(\text{perturbed}) / t_{ign}(\text{baseline})) \qquad (3)$$

A positive coefficient denotes an increase in the ignition delay time and a negative coefficient denotes a decrease in ignition delay. An inspection of Table 2 shows that the chain branching reaction 1 and the chain terminating reactions 9a, 9b and 9c [54] are, as expected, of greatest importance. An increase of a factor of two in the chemical kinetic rate of reactions 9b and 9c resulted in a factor of ~20 increase to the ignition delay time at 1000 K. The uncertainty factor associated with these reactions is a factor of three for the 300 K - 2000 K temperature range [9]. The perturbed change in the kinetic rate for $H + O_2 + M = HO_2 + M$ (M = N_2, H_2) is well within the uncertainty factor established for this reaction and demonstrates the need for further kinetic rate studies involving this important chain terminating process.

The $O + OH = O_2 + H$ reaction showed a factor of ~5 decrease in the ignition delay time at 1000 K and its kinetic rate is relatively well-known. For temperatures at 1111 K, reaction 1 exhibited the highest sensitivity to the ignition delay time with reactions 9b and 9c showing a minor influence at this higher temperature.

Although the ignition delay time is very sensitive to reactions 1, 9a, 9b, and 9c, this study also examined the sensitivity of the ignition delay times to other reaction rates. Chain reactions such as $O + H_2 = OH + H$ and $H + HO_2 = OH + OH$ reduce ignition delay by producing reactive radicals OH and H. The $H + HO_2 = H_2 + O_2$ reaction is chain terminating at 1000 K as it consumes a reactive H-atom plus an unreactive HO_2 radical to make stable products. However, at 1111 K, the reverse rate of this reaction begins to become important as the reactants H_2 and O_2 produce H and HO_2 radicals at these very short residence times.

SUMMARY

Detailed and global chemical kinetics for hydrogen-air mixtures have been validated against data derived from flame propagation, flame structure and shock tube ignition delay time studies. The chemical kinetic mechanism for the detailed reaction model was critically reviewed and well-simulated the experimental measurements. A global rate expression validated against hydrogen-air laminar flame speeds was developed for the single-step reaction $H_2 + 1/2\ O_2 = H_2O$.

Acknowledgement

This work was carried out under the auspices of the U.S. Department of Energy by the Lawrence Livermore National Laboratory under contract No. W-7405-ENG-48.

REFERENCES

1. D.A. Masten, R.K. Hanson, and C.T. Bowman, J. Phys. Chem., vol. 94, p. 7119, 1990.
2. J.V. Michael, Prog. Energy Comb. Sci., vol. 18, p. 327, 1992.
3. M.S. Wooldridge, R.K. Hanson, and C.T. Bowman, Int. J. Chem. Kin.,vol. 26, p.389, 1994.
4. J.W. Sutherland, P.M. Patterson, and R.B. Klemm, J. Phys. Chem., vol. 94 , p. 2471, 1990.
5. G. Dixon-Lewis, Archivum Combustionis, vol. 4, p. 279, 1984.
6. W. Tsang, and R.F. Hampson, J. Phys. Chem. Ref. Data, vol. 15, p. 1095, 1986.
7. C.J. Cobos, H. Hippler, and J. Troe, J. Phys. Chem., vol. 89, p. 342, 1985.
8. J. Warnatz, *Combustion Chemistry*; chap. 5, W.C. Gardiner (ed.), Springer-Verlag, New York, 1984.
9. D.L. Baulch, C.J. Cobos, R.A. Cox, C. Esser, P. Frank, Th. Just, J.A. Kerr, M.J. Pilling, J. Troe, R.W. Walker, and J. Warnatz, J. Phys. Chem. Ref. Data,vol. 21,p. 411, 1992.
10. H. Hippler, J. Troe, and J. Willner, J. Chem. Phys., vol. 93, p. 1755, 1990.
11. R.J. Kee, F.M. Rupley, and J.A. Miller, Sandia National Laboratory, Albuquerque, N.M., SAND87-8215B, 1987.
12. R.A. Yetter, F.L. Dryer, and H. Rabitz, Comb. Science Tech., vol. 79, p. 97, 1991.
13. W. Wong, and D.D. Davis, Int. J. Chem. Kin., vol. 6, p. 401, 1974.
14. K.L. Carleton, W.J. Kessler, and W.J. Marinelli, J. Phys. Chem., vol. 93, p. 1018, 1989.
15. K.J. Hsu, K.J., S.M. Anderson, J.L. Durant, and F. Kaufman, J. Phys. Chem., vol. 93, p. 282, 1989.
16. A.N. Pirraglia, J.V. Michael, J.W. Sutherland, and R.B. Klemm, J. Phys. Chem., vol. 93, p. 282, 1989.
17. Gay, A.; and Pratt, N.H.: *Proceedings of Eighth (International) Shock Tube Symposium*, p. 39, Chapman and Hall, London, 1971.
18. Pamidimukkala, K.M.; and Skinner, G.B.: *Thirteenth (International) Symposium of Shock Tubes and Waves*, p. 585, SUNY Press, Albany, New York, 1981.
19. M.A.A. Clyne, and B.A. Thrush, Proc. R. Soc. London, Ser. A, vol. A275, p. 559, 1963.
20. O.J. Nielsen, A. Sillesen, K. Luther and J. Troe, J. Phys. Chem., vol. 86,p. 2929, 1982.
21. V.F. Kochubei, and F.B. Moin, Ukr. Khim. Zh., vol. 39, p. 888, 1973.
22. M.W. Slack, Comb. Flame, vol. 28, p. 241, 1977.
23. J. Peeters, and G. Mahnen, *Fourteenth Symposium (International) on Combustion*, p. 133, The Combustion Institute, Pittsburgh, 1973.
24. L.F. Keyser, J. Phys. Chem., vol. 90, p. 2994, 1986.
25. R.R. Baldwin, and R.W. Walker, R.W., *Seventeenth Symposium (International) on Combustion*, p. 525, The Combustion Institute, Pittsburgh,1979.
26. T. Koike, Bull. Chem. Soc. Jpn., vol. 62, p. 2480, 1989.
27. R.G. Gilbert, K. Luther, and J. Troe, Ber. Bunsenges. Phys. Chem., vol. 87, p. 169, 1983.
28. R. Zellner, F. Ewig, R. Paschke, and H. Wagner, J. Phys. Chem., vol. 92, p. 4184, 1988.
29. J. Troe, Ber. Bunsenges. Phys. Chem., vol. 73, p. 946, 1969.
30. J. Troe, J. Chem. Soc. Faraday Trans., vol. 90, p. 2303, 1994.
31. L. Brouwer, C.J. Cobos, J. Troe, H.R. Dubai, and L.L. Crim, J. Chem. Phys., vol. 86, p. 6171, 1987.
32. V.Y. Basevich, S.M. Kogarko, and O.Y. Berezin, Izv. Akad. Nauk SSR, vol. 9, p. 1986, 1979.
33. E.A. Albers, H. Hoyerman, H.G. Wagner, and J. Wolfrum, *Thirteenth Symposium (International) on Combustion*, p. 81, The Combustion Institute, Pittsburgh, 1971.
34. H. Hippler, and J. Troe, Chem. Phys. Lett., vol. 192, p. 333, 1992.

35. R.R. Baldwin, and L. Mayor, Trans. Faraday Soc., vol. 57, p. 1578, 1960.
36. R.R. Baldwin, and D. Bratten, *Eighth Symposium (International) on Combustion*, p. 110, The Combustion Institute, Pittsburgh, 1962.
37. M. Kurylo, J. Murphy, G. Haller, and K. Curnett, Int. J. Chem. Kin., vol. 14, p. 1149, 1982.
38. L. F. Keyser, J. Phys. Chem., vol. 84, p. 1659, 1980.
39. F. Takahashi, M. Mizomoto, and S. Ikai, *Alternative Energy Sources III*, vol. 5 Nuclear Energy / Synthetic Fuels, p. 447, T. Nejat Veziroglu (ed.), McGraw-Hill, New York, 1983.
40. G.W. Koroll, R.K. Kumar, and E.M. Bowles, Comb. Flame, vol. 94, p. 330, 1993.
41. C. M. Vagelopoulos, F.N. Egolfopoulos, and C.K. Law, *Twenty-Fifth Symposium (International) on Combustion*, p. 1341, The Combustion Institute, Pittsburgh, 1995.
42. C.K. Wu, and C.K. Law, *Twentieth Symposium (International) on Combustion*, p. 1941, The Combustion Institute, Pittsburgh, 1984.
43. D.R. Dowdy, D.B. Smith, S.C. Taylor, and A. Williams, *Twenty-Third Symposium (International) on Combustion*, 325, The Combustion Institute, 1990.
44. F.N. Egolfopoulos, and C.K. Law,*Twenty-Third Symposium (International) on Combustion*, p. 333, The Combustion Institute, Pittsburgh, 1990.
45. T. Iijima, and T. Takeno, Comb. Flame, vol. 65, p. 35, 1986.
46. M. Berman, Sandia National Laboratory, Albuquerque, N.M., SAND84-0689, 1984.
47. M. Matalon, and B.J. Matkowsky, J. Fluid. Mech., vol. 124, p. 239, 1982.
48. C.K. Law, *Twenty-Second Symposium (International) on Combustion*, p. 1381, The Combustion Institute, Pittsburgh, 1988.
49. R.J. Kee, J.F. Grcar, M.D. Smooke, and J.A. Miller, Sandia National Laboratory, Albuquerque, N.M., SAND85-8240, 1985.
50. R.J. Kee, G. Dixon-Lewis, J. Warnatz, M.E. Coltrin, and J.A. Miller, Sandia National Laboratory, Albuquerque, N.M., SAND86-8246, 1986.
51. C.M. Lund, Lawrence Livermore National Laboratory Report UCRL-52504, 1978.
52. J. Vandooren, and J. Bian, *Twenty-Third Symposium (International) on Combustion*, p. 341, The Combustion Institute, Pittsburgh, 1990.
53. A.E. Lutz, R.J. Kee, and J.A. Miller, Sandia National Laboratory, Albuquerque, N.M.; SAND87-8248, 1988.
54. The HO_2 radical produced in reaction 9 exhibits very low reactivity and, therefore, reaction 9 behaves more as a chain terminating reaction than a chain propagating reaction.